Heliyon 6 (2020) e03593

Contents lists available at ScienceDirect

Heliyon

journal homepage: www.cell.com/heliyon

Research article

Pyrrolizidine alkaloids in bee pollen identified by LC-MS/MS analysis and colour parameters using multivariate class modeling

Luciana De Jesus Inacio [a], Roberta Merlanti [a,*], Lorena Lucatello [a], Vittoria Bisutti [b], Barbara Contiero [b], Lorenzo Serva [b], Severino Segato [b], Francesca Capolongo [a]

[a] Department of Comparative Biomedicine and Food Science, University of Padova, 35020, Legnaro, PD, Italy
[b] Department of Animal Medicine, Production and Health, University of Padova, 35020, Legnaro, PD, Italy

ARTICLE INFO

Keywords:
Food science
Food safety
Public health
Toxicology
Analytical chemistry
Bee pollen
Pyrrolizidine alkaloids
LC-MS/MS
CIE-L*a*b* colour coordinates
Receiver operating characteristic
Canonical discriminant analysis

ABSTRACT

Toxic pyrrolizidine alkaloids (PAs) and their N-oxides (PANOs) can be present in bee pollen depending on the plants visited by bees. A liquid chromatography-mass spectrometry (LC-MS/MS) method was developed and validated to monitor 17 PAs/PANOs in 44 bee pollens. The CIE-L*a*b* colour coordinates with the specular component either included or excluded were recorded in pellets and ground aliquots. Lightness (L*) and yellowness (b*) of ground bee pollen were significantly correlated to PAs/PANOs content. The L* and b* cut-offs sorted by a receiver operating characteristic analysis to predict PAs/PANOs presence showed a significant increase in the relative risk to detect amounts higher than 84 μg kg^{-1}. Two supervised canonical discriminant analyses confirmed that pollen without PAs could be distinguished from those containing PAs/PANOs. The data suggest that instrumental colour coupled with supervised models could be used as a screening test for PAs/PANOs in bee pollen, before the confirmatory LC-MS/MS analysis.

1. Introduction

Bee pollen comprises a mixture of flower pollen, nectar and bee salivary secretions; it is used by the bees to feed their larvae. It contains carbohydrates, proteins, lipids, vitamins, minerals and other bioactive compounds, such as polyphenols, that may exert antioxidant, anti-inflammatory, antifungal, antibacterial and anti-allergic actions, among others (Campos et al., 2008; Campos et al., 2010; Denisow and Denisow-Pietrzyk, 2016). Bee pollen is a natural product and has nutritional and therapeutic properties. Thus, its consumption as a food supplement has recently increased, along with its application in the food industry, where colour and particle size are important characteristics for production (Costa et al., 2017; Salazar-González et al., 2018). However size, shape, colour and composition of bee pollen vary depending on factors like the botanical sources visited by the honeybees, geographic origin and the season of harvest (Denisow and Denisow-Pietrzyk, 2016; Kieliszek et al., 2018; Salazar-González et al., 2018). Pollen grains can have different colours, including yellow, grey-white, orange, reddish, greenish or blue, that indicate the variety of plant species from which the pollen was collected (Kieliszek et al., 2018). As reported above, the colour of bee pollen is also influenced by the presence of pigments such as flavonoids (mainly quercetin and kaempferol) and carotenoids like lutein and beta-carotene (Gardana et al., 2018). Moreover, changes in pollen colour and composition might depend on the processing and storage conditions. Fresh bee pollen contains between 20 and 30% of water, which favours the proliferation of microorganisms and chemical/enzymatic reactions that result in deterioration of the product kept at room temperature. Thus, to preserve its quality and increase its shelf life, bee pollen is subjected to a dehydration process that reduces its water content to 4–8% (Campos et al., 2008). On the other hand, this process can lead to a loss of some nutritious compounds like beta-carotene and vitamin E (Pereira De Melo & De Almeida-Muradian, 2010).

In addition to the compounds that provide beneficial effects to human health, natural toxins, such as mycotoxins (Kostić et al., 2019) and pyrrolizidine alkaloids (PAs), may be present in bee pollen and other bee products. PAs and their N-oxides (PANOs) are produced by plants from the families Asteraceae (tribes *Senecioneae* and *Eupatorieae*), Boraginaceae (all genera, e.g., *Echium* and *Heliotropium*) and Fabaceae (genus *Crotalaria*; Hartmann, 1999; Stegelmeier et al., 1999). Some of

* Corresponding author.
E-mail address: roberta.merlanti@unipd.it (R. Merlanti).

https://doi.org/10.1016/j.heliyon.2020.e03593
Received 17 January 2020; Received in revised form 13 February 2020; Accepted 11 March 2020

these plants are reportedly toxic to mammals, including humans and livestock (Edgar et al., 2011; Molyneux et al., 2011).

Humans are exposed to PAs/PANOs mainly through the consumption of herbal tea, herbal remedies or dietary supplements prepared with plants that contain them (Chen et al., 2017). Many publications have reported the presence of PAs/PANOs in honey and bee pollen, but their concentrations in the latter is much higher (Boppré et al., 2008; Dübecke et al., 2011; Kempf et al., 2010; Mulder et al., 2015). Despite the recognised toxic effects of PAs and reported cases of human and animal poisoning, there are currently no European regulations specifying maximum residue limits in food and feed (Picron et al., 2019). Thus, the Panel on Contaminants in the Food Chain (CONTAM Panel) of the European Food Safety Authority (EFSA)—based on the available data on the occurrence and toxicity of PAs—recommended that the daily intake should not exceed 0.007 μg kg^{-1} body weight (b.w.), in order to avoid carcinogenic effects. This dose was calculated considering a margin of exposure (MOE) of 10000 and a benchmark dose lower confidence limit for a 10% excess cancer risk ($BMDL_{10}$) of 70 μg kg^{-1} b.w. per day (BfR, 2011; COT, 2008; EFSA, 2011). The EFSA also recommended the development of more sensitive and selective analytical methods for quantification of PAs in different matrices (EFSA, 2011, 2017).

Identification and quantification of PAs/PANOs in food matrices, such as bee pollen, have mostly been performed by high performance liquid chromatography coupled to mass spectrometry (HPLC-MS). This method detects very low concentrations of individual PAs/PANOs with high sensitivity and selectivity by target analysis (Mulder et al., 2015; Picron et al., 2019). Unlike honey, there is a lack of information about the determination of these natural toxins in pollen (Boppré et al., 2008; Dübecke et al., 2011; Kast et al., 2018; Kempf et al., 2010). Furthermore, to the best of our knowledge, only a few studies detected PAs/PANOs using a validated liquid chromatography–tandem mass spectrometry (LC-MS/MS) method, even though a limited number of samples was analysed and the type of blank matrix used to validate the method is unclear (Mulder et al., 2015; Picron et al., 2019).

Given that the presence of PAs/PANOs in food may pose a risk to human and animal health, it would also be useful to develop fast, simple and non-destructive screening methods that allow the assessment of contaminated matrices that has to be confirmed by more precise but expensive analysis such as LC-MS/MS. In the literature, a colorimetric assay (Mattocks and Jukes, 1987) and nuclear magnetic resonance (NMR; Nuringtyas et al., 2012) have been reported as rapid techniques to evaluate the qualitative profile of PAs/PANOs in plant extracts, while an enzyme-linked immunosorbent assay (ELISA) has been applied to honey and feed (Oplatowska et al., 2014). These analytical methods have some disadvantages, including complicated sample preparation, relative low sensitivity and—for ELISA—the presence of some cross-reactivity inhibiting the detection of target PAs.

Among the physicochemical analyses available for pollen characterisation, the lightness (L*), redness (a*) and yellowness (b*) colorimetric parameters (*Commission Internationale de l'Éclairage*; CIE, 1976) have rarely been used despite colour being one of the most observed quality traits by consumers (Salazar-González et al., 2018). The CIE-L*a*b* parameters of bee pollen reportedly have a relationship with the total phenolic content, calcium and magnesium amounts (De-Melo et al., 2018) and vitamin E content (De-Melo et al., 2016). In this context, the aim of this study was to evaluate whether instrumental CIE-L*a*b* colour coordinates could represent a reliable and high throughput tool to screen bee pollen samples in regards to the presence of 17 PAs/PANOs markers. To achieve this purpose, the first step was to develop and validate an LC-MS/MS method, according to the Commission Decision 2002/657/EC (European Commission, 2002), to identify and quantify 17 PAs in pollen. The protocol was performed as described in a previous study of six PAs in honey (Lucatello et al., 2016), with slight modifications. In the sample preparation, a delipidation step was added as bee pollen contains lipids that can interfere with the LC-MS analysis, and the reduction step of PANOs was not necessary since the method presented includes the respective N-oxides of the PAs analysed.

The hypothesis that a colorimetric method might be useful for quickly assessing the presence of PAs in bee pollen was tested by means of the application of two multivariate class modelling analyses, namely the receiver operating characteristic (ROC) and canonical discriminating analysis (CDA).

2. Materials and methods

2.1. Bee pollen sampling and experimental design

The bee pollen samples ($n = 44$) were acquired from local market and online stores. Thirty samples were produced in different Italian regions, while 14 came from EU/non-EU countries. All samples were purchased in the dehydrated form that means a water content $< 6\%$ based on the guidelines suggested by Campos et al. (2008). The samples were kept in a dark, cool and dry place, pending LC-MS/MS analysis in ground, not frozen samples. The bee pollen instrumental colour was instead analysed in pellets and ground after a grinding process (physical form fixed effect). Moreover, the colour of pellets and ground aliquots was analysed before and after a 1-month period of storage at -20 °C (preservation method fixed effect).

2.2. Chemicals and reagents

Echimidine (Echi, 97% purity), echimidine N-oxide (Echi NO, 97% purity), heliotrine (Helio, 91% purity), heliotrine N-oxide (Helio NO, 91% purity), lycopsamine (Lyco, 80% purity) and lycopsamine N-oxide (Lyco NO, 80% purity) were obtained from PhytoLab GmbH & Co. KG (Vestenbergsgreuth, Germany); senecionine (Senec, 99% purity), senecionine N-oxide (Senec NO, 99% purity), seneciphylline (Senep, 94% purity) and seneciphylline N-oxide (Senep NO, 94% purity) were from Carl Roth & Co. KG (Karlsruhe, Germany); indicine-N-oxide (Indi NO, 99% purity), intermedine (Inter, 99% purity), jacobine (Jaco, 98% purity), jacobine N-oxide (Jaco NO, 98% purity), retrorsine (Retro, 90% purity), retrorsine N-oxide (Retro NO, 96.0% purity) and senkirkin (Senk, 98% purity) were procured from Phytoplan (Heidelberg, Germany); caffeine (internal standard, IS, 98% purity) was from Sigma-Aldrich (Steinheim, Germany).

Methanol (MeOH) and sulphuric acid (H_2SO_4) were from Carlo Erba reagents (Milan, Italy). Ammonia (NH_3, 28% purity) was from VWR Chemicals. Formic acid (FA, 98% purity) was from Sigma-Aldrich. All reagents were of analytical grade. Pure water was obtained from a Milli-Q water purification system Purelab Classic, ELGA Lab Water (High Wycombe, UK). Strong cation exchange polymeric solid-phase extraction (SPE) cartridges (Bond Elut Plexa PCX, 200 mg/6 mL) and Captiva regenerated cellulose 0.22 μm syringe filters were acquired from Agilent Technologies (CA, USA).

2.2.1. Preparation of standard solutions

Stock solutions of PAs, PANOs and caffeine (IS) were prepared at a concentration of 1000 μg mL^{-1} in MeOH and stored at 4 °C in amber glass. Working solutions, containing all 17 PAs/PANOs were prepared by serial dilution from the concentrated Mix (10 μg mL^{-1} in MeOH), using a blend of 0.1% FA in MeOH (20%) and 0.5% FA in H_2O (80%) to obtain the final concentrations of 0.02, 0.05, 0.10, 0.2, 0.5, 1, 2 and 5 μg mL^{-1}.

2.3. Sample preparation for LC-MS/MS analysis

Approximately 30 g of bee pollen was ground and homogenised using a food mixer. To 2.5 g of ground bee pollen, 15 mL of 0.05 M H_2SO_4 was added, and the samples were shaken for 10 min in a mechanical shaker. After adding 10 mL of *n*-hexane, the samples were shaken again for 10 min, and then centrifuged at 3000 g for 10 min at room temperature. The organic layer was discarded, and the aqueous layer of each sample was

Table 1. MS/MS data acquisition for PAs, PANOs and IS and their respective retention times.

Analytes	RT (min)	Precursor ion $[M + H]^+$ (m/z)	CE (%)	Product ions MS^2 (m/z)
Indicine N-oxide (Indi NO)	5.6	316	33	298, 272, 226, 172, 138
Jacobine (Jaco)	6.0	352	25	308, 280, 262, 155, 120
Lycopsamine (Lyco)	6.3	300	28	156, 138, 120, 94
Intermedine (Inter)	6.4	300	28	138, 120, 94
Retrorsine N-oxide (Retro NO)	7.5	368	28	340, 338, 246, 220, 118
Jacobine N-oxide (Jaco NO)	9.0	368	30	324, 296
Lycopsamine N-oxide (Lyco NO)	9.0	316	33	272, 226, 172, 138, 94
Retrosine (Retro)	11.5	352	25	324, 276, 138, 120
Caffeine (IS)	12.2	195	35	138
Seneciphylline (Senep)	12.5	334	25	306, 280, 138, 120
Heliotrine (Helio)	12.7	314	23	156, 138, 120, 96
Seneciphylline N-oxide (Senep NO)	13.6	350	30	332, 322, 208, 246, 118
Heliotrine N-oxide (Helio NO)	14.2	330	30	298, 172
Senecionine (Senec)	15.1	336	25	308, 290, 138, 120
Senecionine N-oxide (Senec NO)	15.4	352	25	324, 246, 220, 118
Echimidine N-oxide (Echi NO)	16.5	414	30	396, 352, 254
Echimidine (Echi)	16.6	398	40	380, 336, 220, 120
Senkirkine (Senk)	16.9	366	25	348, 168, 150, 122

RT: retention time; CE: collision energy; IS: internal standard; _ quantifier ion.

applied onto strong cation exchange polymeric SPE cartridges (Bond Elut Plexa PCX, 200 mg/6 mL). The SPE extraction was performed as described in Lucatello et al. (2016).

2.4. Chromatographic and mass spectrometric conditions

The analyses were performed on a LC-MS/MS system that comprised an Accela 600 HPLC pump with a CTC automatic injector (Thermo Fisher Scientific, San Jose, CA, USA) coupled to an LTQ XL ion trap mass spectrometer (Thermo Fisher Scientific) equipped with an electrospray ionisation source (HESI-II probe) operating in the positive ion mode. The chromatographic separation of the 17 PAs/PANOs was carried out using a Hypersil GOLD C18 analytical column (100 mm × 2.1 mm, 1.9 μm; Thermo Fisher Scientific) and a mobile phase consisted of solvent A (0.1% formic acid in water) and solvent B (0.1% formic acid in MeOH). The elution gradient was set as follows: the solvent B was set at 10% from 0 to 4 min, increased to 15% from 4 to 4.5 min and held until 9 min, followed by a linear increasing to 40% from 9 to 14 min, and then brought to 80% from 14 to 16.5 min. Subsequently, solvent B was reduced back to 10% in 0.5 min and held until 20 min to reconditioning the column.

The injection volume, the flow rate and the tuning parameters applied were those reported in Lucatello et al. (2016).

For all the PAs and PANOs, the precursor ions, product ions, collision energies and retention times obtained are shown in Table 1. The Xcalibur software (version 2.1) was used for system control, data acquisition and analysis.

2.5. LC-MS/MS method validation

The analytical method was validated using an in-house model in agreement with the European Commission Decision 2002/657/EC. The following analytical parameters were evaluated: specificity ($n = 20$ blank pollens); linearity (six different calibration curves—on six different days) in the final concentrations of 0, 0.4, 1, 2, 4, 10, 20, 40 and 100 μg kg^{-1}; apparent recovery (Rapp) on three concentration levels (2, 10 and 40 μg kg^{-1}), with six replicates at each level, on three different days. Precision (within-day repeatability, RSDr, and within-laboratory reproducibility, RSDR) and limit of quantification (LOQ) have been assessed. Finally, absolute recovery (ABS REC%) was calculated by dividing the slope of the calibration curves, obtained with the blank matrix spiked with PAs/PANOs before the extraction, by the slope of the calibration curves obtained with blank matrix spiked after the extraction procedure (equation 1).

Absolute recovery calculation:

$$ABS\ REC\% = \frac{SLOPE_{spiked\ pre-extraction}}{SLOPE_{spiked\ post-extraction}}\ x\ 100 \quad (1)$$

The matrix effect (ME) was calculated by dividing the slope of the calibration curves obtained with the samples spiked after extraction by the slope of the calibration curves prepared with the standards in mobile phase, in the absence of matrix (equation 2). If there is no matrix effect, the values range from -20 to +20%. Otherwise, it is considered a medium matrix effect with values between 20 and 40% and -20 and -40%, and a strong matrix effect with values more than ±40% (Ferrer et al., 2011).

Matrix effect calculation:

$$ME\% = \left(\frac{SLOPE_{spiked\ post-extraction}}{SLOPE_{standard}} - 1\right)\ x\ 100 \quad (2)$$

2.6. Instrumental colour analysis

The CIE-L*a*b* colour coordinates were determined in six replicates of both pellets and ground bee pollen aliquots in dark conditions using a Konica Minolta CD-600 visible spectrophotometer (Konica Minolta Sensing, Inc., Japan). The instrument was calibrated against a white standard plate using an 8-mm diameter measuring aperture and an illuminant D65 (equivalent to natural daylight), set at 10° for the observation angle. The L*a*b* colour coordinates were expressed according to the measurement modalities related to whether the specular component was included or excluded, namely the SCI and SCE modes, respectively. In the SCE mode of colour measurement only the diffuse light is considered, which is better connected with the human visual evaluation as it takes into account the surface of the sample and its related effects. Instead, in the SCI mode total reflectance is obtained (sum of the diffuse and specular light),

which corresponds to the colour of the sample regardless the surface conditions. The reflectance spectra were registered within the visible region ($\lambda = 400–700$ nm) at constant intervals ($\lambda = 10$ nm).

2.7. Statistical analysis

All the statistical analyses were performed using the SAS 9.4 software (SAS Institute Inc., Cary, NC, USA) and MedCalc (version 17.6, MedCalc Software bvba). Data normality was assessed using the Shapiro-Wilk test (PROC UNIVARIATE) and considering a threshold of 0.90 as a limit for a normal distribution. Bee pollen colour coordinates were submitted to ANOVA (PROC GLM), adopting a linear model that considered the fixed effects physical form of the matrix (pellets vs. ground) and preservation method (not frozen vs. frozen) and their interaction. The hypothesis of the linear model on normal distribution of the residuals was graphically assessed.

Due to the non-normally distributed PAs/PANOs data, a linear correlation analysis (Spearman's rank test, r_{sp}) was carried out between the six colour coordinates (L*, a* and b* as SCI and SCE mode) and the total PAs/PANOs content. A ROC analysis was performed on ground, not frozen samples to find a significant threshold on the SCI- and SCE-L*a*b* measures related to two gold standards. The first gold standard was the PAs/PANOs content, which was dichotomised in two classes according to the LOQ threshold (LOQ-TR): LOQ-TR < 0.4 μg kg^{-1}, absence vs. LOQ-TR ≥ 0.4 μg kg^{-1}, presence. The second gold standard was dichotomised in two classes according to the EFSA safety threshold (EFSA-TR) of 84 μg kg^{-1}: EFSA-TR < 84 μg kg^{-1}, compliant vs. EFSA-TR ≥ 84 μg kg^{-1}, non-compliant.

The ROC analysis is the plot of sensitivity and 1 – specificity of a test, and the area under ROC curve (AUC) represents the accuracy of the method. Applying the Youden index, a criterion that maximises the sensitivity and specificity, significant cut-off values for SCI- and SCE-L* and b* were found using both gold standards LOQ-TR and EFSA-TR.

A risk analysis was conducted to calculate the relative risk (RR) to detect a level of PAs/PANOs over 84 μg kg^{-1} if the colour coordinates were under the cut-offs found in the ROC analysis. Data were analysed using a 2 x 2 contingency table and submitted to a chi-square (χ^2) test to assess the association between the level of PAs/PANOs and the SCI- and SCE-L* and b* parameters (both dichotomised).

A double stepwise discriminant analysis (PROC STEPDISC) was applied to the 31 reflectances of the optical light of the spectrophotometer at specific wavelength variables (from λ_{400} to λ_{700}, with a 10 nm interval) to identify the ones that significantly affected the variability of the alkaloids. The first stepwise considered three quantitative PAs/PANOs (μg kg^{-1}) classes: absence, PAs/PANOs <0.4; compliant, $0.4 \leq$ PAs/PANOs < 84; non-compliant, PAs/PANOs ≥ 84. The second one involved five qualitative PAs/PANOs classes: absence (without the 17 monitored PAs/PANOs); lycopsamine-type (L-type: Echi, Echi NO, Indi NO, Inter, Lyco and Lyco NO); senecionine-type (S-type: Jaco, Jaco NO, Retro, Retro NO, Senec, Senec NO, Senep, Senep NO and Senk); lycopsamine-senecionine-type (LS-type); and lycopsamine-senecionine-heliotrine-type (LSH-type; H-type: Helio and Helio NO). Two CDAs (PROC CANDISC) were performed on the selected predictive reflectance variables of the two stepwise analyses. Two confusion matrices were calculated. Each samples was assigned to an experimental class according to the shortest square Mahalanobis distance generated by the relative CDA. As reported in Bisutti et al. (2019), the goodness of the classifications for CDA models was estimated by means of some descriptive statistics, including sensitivity, specificity, accuracy, precision and the Matthews correlation coefficient (MCC).

3. Results and discussion

3.1. LC-MS/MS method validation

One of the aims of this work was to develop an LC-MS/MS method that could evaluate the PAs/PANOs profile in bee pollen samples. This protocol was performed as described by Lucatello et al. (2016) for honey, with slight modifications related to the extraction method and the elution gradient. The method was fully validated to monitor 17 PAs/PANOs in this new matrix, consistent with the European Commission Decision 2002/657/EC. Certified bee pollen samples without PAs/PANOs were not available, and thus willow, chestnut and ivy pollens were mixed and used as a pool of blank pollen for the validation study.

The chromatograms of blank bee pollens and those of the corresponding spiked matrix were compared to verify the specificity. No significant interfering signals were observed at the retention time of each PA/PANO studied, so the method was able to differentiate between target analytes and other compounds.

The linearity was successfully verified over the working range considered for PAs/PANOs (0.4–100 μg kg^{-1}). Indeed, the calculated R^2 was > 0.99 for most of the compounds except Echi and Senk, for which the R^2 was 0.96 and 0.98, respectively. No statistically significant difference ($P > 0.05$) among the slopes and intercepts of each calibration curve was detected (Table 2).

Table 2. Calibration curve linear range, slope and intercept with standard deviation (SD), variation coefficient (R^2), limits of quantification (LOQ).

Analyte	Linear Range (μg kg^{-1})	Slope ± SD	Intercept ± SD	R^2	LOQ (μg kg^{-1})
Indi NO	0.4–100	0.0161 ± 0.0015	0.0067 ± 0.0039	0.9988 ± 0.0015	0.4
Jaco	0.4–100	0.0071 ± 0.0004	0.0032 ± 0.0012	0.9992 ± .00007	0.4
Lyco	0.4–100	0.0091 ± 0.0004	0.0119 ± 0.0064	0.9963 ± 0.0021	0.4
Inter	0.4–100	0.0184 ± 0.0003	0.0268 ± 0.0159	0.9941 ± 0.0061	0.4
Retro NO	0.4–100	0.0014 ± 0.0001	0.0023 ± 0.0003	0.9981 ± 0.0022	0.4
Jaco NO	0.4–100	0.0121 ± 0.0014	0.0149 ± 0.0046	0.9993 ± 0.0005	0.4
Lyco NO	0.4–100	0.0143 ± 0.0014	0.0057 ± 0.0049	0.9992 ± 0.0006	0.4
Retro	0.4–100	0.0066 ± 0.0003	0.0020 ± 0.0006	0.9994 ± 0.0011	0.4
Senep	0.4–100	0.0066 ± 0.0006	0.0028 ± 0.0014	0.9995 ± 0.0007	0.4
Helio	0.4–100	0.0394 ± 0.0041	0.0107 ± 0.0065	0.9997 ± 0.0004	0.4
Senep NO	0.4–100	0.0019 ± 0.0002	0.0006 ± 0.0004	0.9992 ± 0.0007	0.4
Helio NO	0.4–100	0.0474 ± 0.0023	0.0135 ± 0.0080	0.9993 ± 0.0008	0.4
Senec	0.4–100	0.0141 ± 0.0010	0.0724 ± 0.0317	0.9985 ± 0.0020	0.4
Senec NO	0.4–100	0.0021 ± 0.0002	0.0010 ± 0.0007	0.9965 ± 0.0031	0.4
Echi NO	0.4–100	0.0200 ± 0.0011	0.0115 ± 0.0077	0.9963 ± 0.0032	0.4
Echi	0.4–100	0.0013 ± 0.0003	0.0012 ± 0.0006	0.9607 ± 0.0156	0.4
Senk	0.4–100	0.0057 ± 0.0003	0.0016 ± 0.0013	0.9848 ± 0.0169	0.4

Table 3. Results for apparent recovery (Rapp), repeatability (RSDr) and reproducibility (RSDR).

Analyte	CN $\mu g\ kg^{-1}$	Day 1 (n = 6)		Day 2 (n = 6)		Day 3 (n = 6)		Inter-day (n = 18)	
		Rapp m (%)	RSDr (%)	Rapp m (%)	RSDr (%)	Rapp m (%)	RSDr (%)	Rapp M (%)	RSDR (%)
Indi NO	2	100.3	1.1	101.1	2.2	101.1	3.5	100.8	2.4
	10	96.0	3.8	106.5	3.3	103.5	4.7	102.0	5.8
	40	99.9	3.6	100.8	2.4	100.9	4.5	98.9	4.5
Jaco	2	99.9	4.7	97.6	3.1	105.4	4.2	101.0	5.1
	10	105.4	1.7	96.4	4.3	108.3	4.7	103.3	6.2
	40	103.9	3.2	99.1	4.2	100.6	5.7	101.2	4.7
Lyco	2	97.0	3.8	103.4	8.8	100.8	5.7	100.4	6.7
	10	84.8	9.2	102.6	11.0	100.9	10.0	96.1	12.9
	40	97.3	4.6	95.8	6.5	100.6	4.9	97.9	5.5
Inter	2	97.9	3.7	98.6	1.7	101.6	4.2	99.3	3.6
	10	90.9	1.6	106.3	9.0	105.6	4.8	101.0	9.3
	40	98.6	2.6	100.6	2.6	102.7	1.5	100.6	2.7
Retro NO	2	102.8	4.1	99.5	4.8	100.7	4.11	101.0	4.3
	10	97.2	4.9	102.9	6.6	108.7	6.14	102.9	7.3
	40	99.9	1.8	101.4	3.1	97.9	6.90	99.73	4.4
Jaco NO	2	96.1	4.6	95.9	3.0	98.2	6.8	98.08	7.2
	10	94.0	6.1	107.3	5.0	105.9	4.2	102.4	7.7
	40	103.5	2.8	99.9	3.8	101.4	3.8	101.6	3.6
Lyco NO	2	96.1	3.0	99.5	5.5	106.2	2.7	100.6	5.6
	10	93.6	3.0	108.4	9.6	102.0	6.9	101.4	9.2
	40	99.2	4.1	103.8	10.8	99.6	2.9	100.9	7.0
Retro	2	103.9	4.2	98.1	8.6	100.9	4.5	101.0	6.1
	10	96.0	4.8	108.9	5.0	97.1	9.4	100.7	8.6
	40	98.2	4.5	105.4	3.3	105.4	4.8	103.0	5.3
Senep	2	101.4	4.1	106.3	4.3	99.9	4.6	102.5	4.9
	10	100.8	4.1	101.8	6.3	108.1	3.4	103.6	5.5
	40	99.8	3.3	102.2	5.9	102.4	3.0	101.5	4.2
Helio	2	95.5	3.8	100.1	5.9	103.3	2.7	99.6	5.2
	10	88.4	6.4	96.2	7.4	105.8	3.5	96.8	9.4
	40	101.3	4.5	105.2	4.8	104.2	3.1	82.8	4.5
Senep NO	2	104.5	3.1	94.8	10.8	102.1	7.4	100.5	8.3
	10	97.4	5.2	102.8	6.6	107.8	7.0	102.7	7.3
	40	99.8	2.8	102.8	3.4	103.6	3.5	102.1	3.5
Helio NO	2	99.8	5.3	100.8	5.1	97.6	4.7	99.4	4.9
	10	101.1	2.3	104.2	9.1	99.4	6.9	101.6	6.7
	40	98.5	2.8	107.1	2.6	102.8	3.7	102.8	4.6
Senec	2	92.2	9.0	105.6	6.3	93.0	7.5	96.9	9.7
	10	104.7	7.9	106.4	10.7	83.8	10.4	107.6	10.5
	40	97.8	7.8	104.9	3.5	100.8	2.7	101.2	5.6
Senec NO	2	92.6	9.1	99.3	5.5	101.0	4.7	97.6	7.2
	10	94.8	4.2	99.9	10.0	91.5	6.7	95.4	8.0
	40	98.5	3.6	103.2	5.1	105.0	2.6	102.2	4.6
Echi NO	2	94.1	7.4	98.2	9.4	106.9	6.8	98.9	9.2
	10	92.9	4.6	107.4	9.0	108.3	3.6	`102.9	9.2
	40	89.6	4.6	101.9	6.4	108.2	12.2	99.9	11.5
Echi	2	88.3	11.2	82.0	12.7	105.7	4.7	92.0	14.3
	10	109.0	10.9	106.4	9.6	102.4	12.2	104.7	10.2
	40	104.6	1.3	91.6	3.9	81.6	9.8	107.1	7.6
Senki	2	99.7	6.9	103.2	5.3	93.9	13.2	98.6	9.4
	10	108.8	1.7	109.4	4.3	109.2	6.4	109.1	4.3
	40	80.1	4.1	84.6	5.2	99.5	10.8	88.1	12.2

Rapp m: average apparent recovery obtained in each day (n = 6 per spiking levels).
Rapp M: average apparent recovery obtained during 3 days (n = 3 × 6 = 18 assays per spiking levels).
RSDr%: percent relative standard deviation under repeatability conditions (n = 6 assays per spiking levels).
RSDR%: percent relative standard deviation under within-laboratory reproducibility conditions (n = 3 × 6 = 18 assays per spiking levels).

In Table 3 the results obtained for apparent recovery (Rapp), repeatability (RSDr) and reproducibility (RSDR) are summarised. The apparent recovery (Rapp%) ranged from 80 to 109%, consistent with the limits established by the Commission Decision 2002/657/EC.

To assess the precision, the RSD% was calculated at the concentration levels of 2, 10 and 40 μg kg^{-1} for each PA/PANO from six replicates analysed on the same day (within-day repeatability, RSDr) and on three different days by distinct operators (within-laboratory reproducibility, RSDR).

All values for RSDr and RSDR were below 13.2 and 14.3%, respectively, proving good precision for all the analytes. A calibration curve was freshly prepared for each analytic session to quantify the PAs/PANOs in unknown samples, and the concentrations were back calculated from the calibration curve. The LOQ was set at 0.4 μg kg^{-1}, which was the lowest level that could be quantified with precision (within 20%) and trueness (80–120%) for each PA/PANO (Table 2).

Absolute recovery (ABS REC%) ranged from 50% (for Echi) to 90.6% (for Lyco NO), and no ME% or medium ME% was calculated for 30 and 35% of tested PAs/PANOs, respectively. For the remaining 35% of the compounds, a strong signal suppression was calculated (values between -47 and -82% for Senep NO and Senk, respectively). The use of internal standard compensated for these matrix effects (Table 4).

Table 4. Absolute recovery (ABS REC%) and matrix effect (ME%) with the relative standard deviation (RSD %) for PAs/PANOs.

Analyte	ABS REC (%)	RSD%*	ME (%)	RSD%**
Indi NO	89.9	6.5	-27.2	12.5
Jaco	76.1	5.9	-40.0	13.9
Lyco	67.8	5.4	-34.7	13.3
Inter	78.2	6.5	-19.3	9.2
Retro NO	87.9	11.0	-24.0	12.3
Jaco NO	84.8	1.5	-60.8	14.9
Lyco NO	90.6	8.9	-16.1	5.1
Retro	87.0	4.9	-14.1	10.9
Senep	81.7	11.8	-12.6	11.0
Helio	81.4	12.5	-1.9	8.3
Senep NO	85.4	15.3	-47.4	12.2
Helio NO	83.2	7.9	-20.2	7.5
Senec	74.4	10.6	-38.8	12.4
Senec NO	86.3	13.1	-55.2	5.7
Echi NO	89.6	4.4	-53.1	7.4
Echi	50.1	9.6	-65.4	12.3
Senk	69.6	9.5	-82.3	2.2

RSD%*: percent relative standard deviation related to ABS REC%.
RSD%:** percent relative standard deviation related to ME%.

3.2. Determination of PAs/PANOs content in bee pollen by LC-MS/MS

The present LC-MS/MS method allows one to monitor 17 PAs/PANOs in bee pollen, which are markers of three groups of those suggested by EFSA (2011): L-type, S-type, and H-type. The marker compounds of the fourth group proposed by EFSA, the monocrotaline-type PAs, synthetised particularly by *Crotalaria* spp. (Fabaceae), was not included in this work because these plant species do not occur in Mediterranean countries and are mainly distributed throughout the tropics.

The validated LC-MS/MS method was applied to the 44 bee pollens to monitor the presence of the selected PAs/PANOs and to define the contamination profile that would provide indirectly useful indications regarding the producing plants. Ten samples (23%) were negative for the target analytes and 34 (77%) contained PAs/PANOs (Figure 1a).

The total PAs/PANOs content in positive samples was in the concentration range of 1.7–3356 μg kg^{-1}, with a mean value of 520 μg kg^{-1}. Considering an average daily consumption of 5 g of bee pollen for an adult weighing 60 kg, and the dose of 0.007 μg PAs kg^{-1} b.w. recommended by EFSA (EFSA, 2011), samples containing up to 84 μg kg^{-1} PAs/PANOs seem to be safe. In 21 bee pollen samples, the total PAs/-PANOs concentration ranged from 142 to 3356 μg kg^{-1}, which is well above the supposed limit of 84 μg kg^{-1} (Figure 1a). Thus, such samples could pose a risk for regular consumers and be considered as "non--compliant", considering the EFSA suggestion.

Among the contaminated bee pollens, 88% contained L-type PAs/PANOs (Figure 1b) between 0.7 and 2078 μg kg^{-1}. The markers Echi and Echi NO contributed the highest average concentrations of 226 and 230 μg kg^{-1}, respectively (Figure 1c). S-type PAs/PANOs were detected in 47% of the samples at levels between 1.7 and 953 μg kg^{-1}. Among the markers monitored from the S-type PAs/PANOs group, Jaco, Jaco NO and Senk were not detected in any samples. Retro NO was less frequent, and a single sample contributed to its high mean concentration (Figure 1c). In turn, the H-type PAs/PANOs (Helio and Helio NO) were present only in four samples at the lowest mean concentration of 3.8 μg kg^{-1} (Figure 1c).

The source of L-type PAs/PANOs could be plants from the genera *Echium*, *Borago*, *Symphytum* or others from the Boraginaceae family.

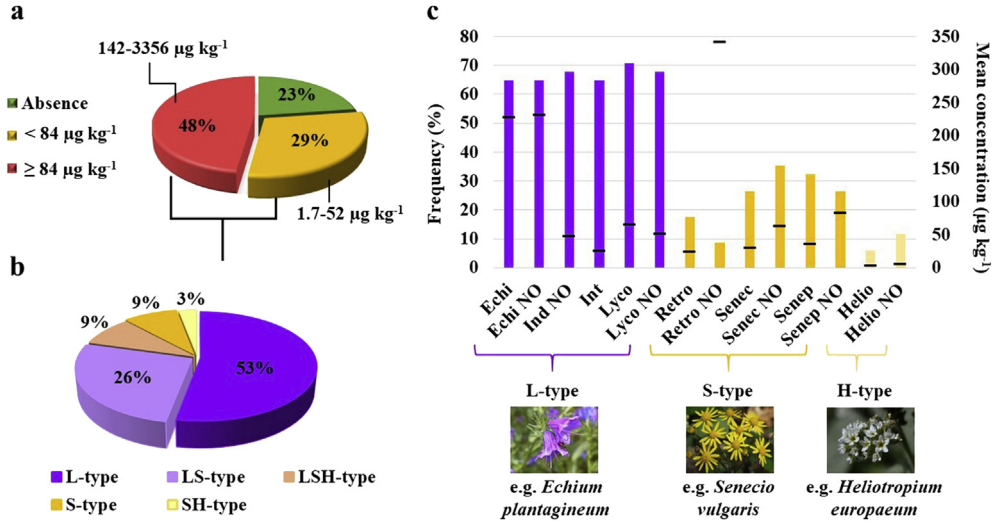

Figure 1. Distribution of the bee pollen samples by total PAs/PANOs content (a) and EFSA groups (b). The mean concentration of individual PAs/PANOs grouped by family type and their respective percentage of detection (c). In chart c, the bars show the frequency (on the left), and the dashes show the mean concentration (on the right) of each PA/PANO detected in the samples.

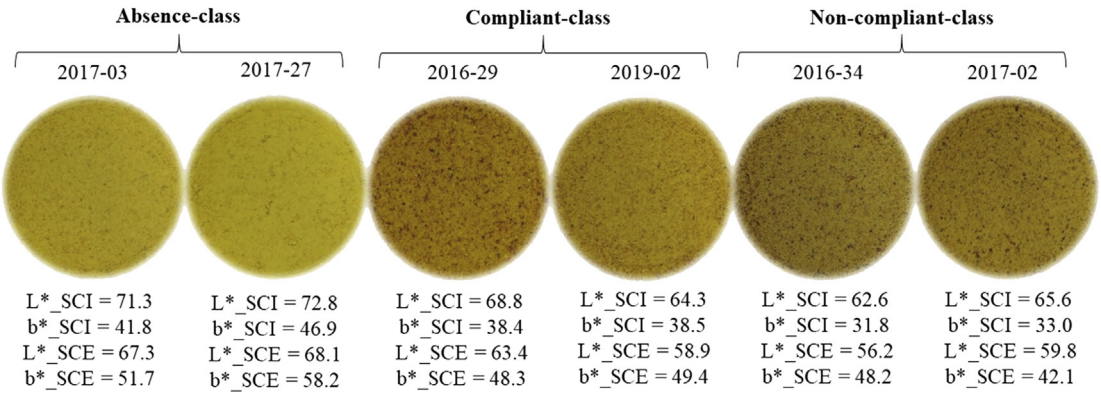

Figure 2. Ground bee pollen samples belonging to one of the three quantitative PAs/PANOs (μg kg^{-1}) classes: (absence, < 0.4; compliant, 0.4 ≤ PAs/PANOs < 84; non-compliant, ≥ 84) with their L* (lightness) and b* (yellowness) colour coordinate values in the spectral component included (SCI) and spectral component excluded (SCE) modes.

Another possible source of L-type PAs/PANOs are species from the tribe *Eupatorieae* (Asteraceae family), such as *Eupatorium.* The presence of S-type PAs/PANOs might be attributed to plants from the tribe *Senecioneae* (Asteraceae), with the genera *Senecio* and *Petasites* among those present in the Mediterranean area. The source of H-type PAs/PANOs are mainly plants from the genus Heliotropium (Boraginaceae), which is also present in Europe (Edgar et al., 2011; EFSA, 2011). Although a comparison of the published total PAs/PANOs contents is hardly possible because the number of targeted compounds always varies (from 6 to 30), one should consider which analytes are found most frequently and at the highest concentrations in bee pollen.

The results obtained in this study are consistent with those reported by Mulder et al. (2015) and Picron et al. (2019). Although those studies used more PAs (28 and 30, respectively), L-type PAs/PANOs were the most widespread analytes detected in bee pollen, followed by S-type PAs/PANOs, while H-type PAs/PANOs were scarcely responsible for the sample contamination. The additional analytes (i.e., erucifoline, erucifoline NO, europine, europine NO, senecivernine and senecivernine NO), monitored by those authors and not considered in this work, were present only in trace amounts and therefore did not contribute significantly to the total PAs/PANOs content. Although Kast and collaborators suggested the inclusion of echivulgarine and its N-oxide in the analysis of pollen from *Echium* to avoid underestimating PAs/PANOs content (Kast et al., 2019), the analytical standards of those molecules are not yet commercially available. Additionally, most samples (68%) containing Echi and Echi NO, which are also typical from *Echium*, the total PAs/PANOs concentration was higher than 84 μg kg^{-1}, and therefore they could be already considered harmful to consumers.

3.3. Instrumental colour analysis

The determination of L*a*b* colour coordinates was performed in order to develop a rapid screening method to predict the contamination of bee pollen with PAs/PANOs, which was the main purpose of this study. In a three-dimensional space model, the coordinates L*, a* and b* represent the lightness, redness and yellowness, respectively. As illustrated in Figure 2, this natural product can be described as very light, quite similar to grey in terms of redness, with a very dark, intense yellow colour. Considering the SCI mode, the combination of the minimum scores (L* = 58, a* = 2 and b* = 28) corresponds to a bright yellow colour, meanwhile, the combination of the maximum (L* = 74, a* = 13 and b* = 46) could be associated with dark yellow-brown tonality. To date there are only a few studies that reported data about the instrumental colour of bee pollen. They showed similar results, with a high range of variation probably due to the complexity of this matrix (De-Melo et al., 2016, 2018; Salazar-González et al., 2018). Moreover, it is interesting to highlight the difference in the colour coordinates between the SCI and SCE modes. In the SCE mode, the b* value (yellowness) was higher, while L* (lightness) was lower. To our knowledge, there are no studies that evaluated colour parameters measured with both SCI and SCE modes in food matrices. Depending on the properties (e.g., surface roughness) and composition of the matrix, a* and b* values can be higher in the SCE mode, as reported by Hosoya et al. (2009), who compared the colour characteristics of different filler type resin composites in SCI and SCE modes. These authors also observed that inclusion of specular component can increase the reflectance percentage at all wavelengths and lead to higher lightness (L*) with the SCI mode.

In both SCI and SCE modes, the L* and b* coordinates were only significantly affected by the fixed effect physical form with the grinding

Table 5. Statistical scores of the receiver operating characteristic (ROC) analysis performed on dry ground bee pollen dataset (n = 44) in discriminating PAs/PANOs (LOQ- and EFSA-threshold) according to L* and b* (specular component included [SCI] or excluded [SCE]) colour parameters.

	AUC ± SEM	95% CI	Cut-off	Sensitivity	Specificity	P
LOQ-threshold (0.4 μg kg^{-1})						
L*_SCI	0.74 ± 0.10	0.58–0.86	67.9	0.71	0.80	0.022
b*_SCI	0.83 ± 0.08	0.69–0.93	39.0	0.91	0.70	<0.001
L*_SCE	0.75 ± 0.10	0.60–0.87	61.8	0.65	0.90	0.016
b*_SCE	0.87 ± 0.08	0.74–0.95	49.7	0.91	0.80	<0.001
EFSA-threshold (84 μg kg^{-1})						
L*_SCI	0.71 ± 0.08	0.55–0.83	67.0	0.71	0.78	0.013
b*_SCI	0.71 ± 0.08	0.55–0.84	38.1	0.81	0.61	0.007
L*_SCE	0.71 ± 0.08	0.55–0.84	61.6	0.76	0.74	0.011
b*_SCE	0.69 ± 0.08	0.53–0.82	49.1	0.86	0.48	0.017

L*, lightness; b*, yellowness; AUC, area under the curve; CI, confidence interval; SEM, standard error of the mean.

Table 6. Outcomes of the relative risk (RR) analysis based on the L* and b* (specular component included [SCI] or excluded [SCE]) cut-offs from the receiver operating characteristic (ROC) analysis.

Cut-off	Samples *n*	Non-compliant bee pollen samples (%)	Chi-square test	P	RR (95% CI)
L*_SCI					
≤67	21	71.4	7.32	0.01	2.71 (1.31–5.73)
>67	23	26.1			
b*_SCI					
≤38	25	64.0	4.73	0.03	2.43 (1.08–5.45)
>38	19	26.3			
L*_SCE					
≤62	24	66.7	6.01	0.01	2.67 (1.19–6.00)
>62	20	25.0			
b*_SCE					
≤49	29	58.6	2.87	0.09	2.20 (0.90–5.37)
>49	15	26.7			

L*, lightness; b*, yellowness; RR, relative risk; Non-compliant, PAs/PANOs ≥ 84 μg kg^{-1}; CI, confidence interval.

process. This effect led to an increase in L* and b* (Table 5), consistent with De-Melo et al. (2016). Regarding the preservation method, a short period of freezing storage did not affect the colour of the thawed bee pollen, probably because the bee pollens were frozen in the dehydrated form. In general, bee pollen is sold on the market after a cleaning and drying process to increase the shelf life (De-Melo et al., 2016; Salazar-González et al., 2018). However, depending on the storage temperature, dried bee pollen can become unfit for consumption and the content of some compounds like vitamins C and E and β-carotene can decrease over time, as reported by Pereira De Melo and De Almeida-Muradian (2010).

Given these results, discriminant models were performed considering the dataset of ground, not frozen bee pollen that is the same form in which the PAs/PANOs were quantified by LC-MS/MS. The first step to define a rapid method to detect the PAs/PANOs using the instrumental colour was related to the assessment of the degree of relationships between the 17 PAs and the instrumental colour coordinates by using the Spearman's rank correlation (r_{sp}) test because the total PAs/PANOs amount was not normal distributed. The results showed moderate and negative relationships with lightness and yellowness. The highest r_{sp} values were detected in ground bee pollens, with the following significant ($P < 0.05$) values: -0.31, L*_SCI; -0.44, b*_SCI; -0.32, L*_SCE; -0.51, b*_SCE. This fact could be related to the matrix homogeneity: ground bee pollen is more homogeneous than pellets, in terms of colour and particle size (Salazar-González et al., 2018).

3.3.1. ROC analysis

In order to determine a correspondence between the PAs/PANOs amount and the colour coordinates, two ROC analyses were performed in accordance with the two chosen gold standards. The first one was the LOQ-TR (< 0.4 μg kg^{-1}, absence vs. > 0.4 μg kg^{-1}, presence) and the second one was the EFSA-TR (< 84 μg kg^{-1}, compliant vs. ≥ 84 μg kg^{-1}, non-compliant). The specific cut-offs for L* and b* determined according to the LOQ-TR or the EFSA-TR seemed to be very similar, but there were relevant differences according to the SCI and SCE measurements for both gold standards (Table 5). However, when using the LOQ-TR, the AUC was slightly higher, data that indicate a more reliable sensitivity and specificity. Thus, in the case of the SCE criterion, the main outcome of the ROC analysis was a definition of a double cut-off (L* = 61.8 and b* = 49.7) that could be used to predict whether PAs/PANOs are present (LOQ-TR) in ground bee pollen, with an accuracy of 0.75 ($P = 0.016$) and 0.87 ($P < 0.001$), respectively (Table 5). AUC values of 0.80–0.90 indicate a reliable discriminant ability, and thus b* (SCI and SCE) seems to be more appropriate to distinguish among bee pollens that contain PAs/PANOs. Chica and Campoy (2012) demonstrated the effectiveness of a ROC-classifier multivariate model coupled with the colour properties for authenticating botanical and geographical origin of bee pollens against fraudulent ones.

3.3.2. Relative risk

In the present study, the RR was calculated using the cut-offs for L* and b* (SCI and SCE) obtained from the ROC analysis. The RR values significantly ranged from 2.43 to 2.71 ($P < 0.05$), except for b*_SCE ($P < 0.10$), which showed the lowest value (Table 6). These results indicated that L* and b* values lower than or equal to their specific cut-offs were associated with a more than double the risk of PAs/PANOs content over 84 μg kg^{-1} in bee pollen. The RR assessment confirmed that the instrumental colour coordinates could be useful in predicting a relevant PAs/PANOs amount for public health, because exposure to these toxins through bee pollen consumption is considerably higher than for other bee products like honey (EFSA, 2011).

3.3.3. Canonical discriminant analysis

To improve the instrumental colour classification performance of the PAs/PANOs classes, CDA algorithms based on both the SCI and SCE colour data were performed. For the quantitative classes, the SCI and SCE results were quite similar, but for the qualitative classes, the SCE ones were more accurate. Thus, only the SCE outcomes were selected for both CDA. These supervised classifier models were used to select—by a forward stepwise procedure—the most informative optical-light reflectance variables associated with the 31 wavelengths (λ = 400–700 nm, with a 10 nm interval) of the spectrophotometer in discriminating the PAs/PANOs classes. For the EFSA-clustering based on the threshold of 84 μg kg^{-1}, which allowed the definition of three quantitative (μg kg^{-1}) classes, namely absence, (< 0.4), compliant (0.4 ≤ PAs/PANOs < 84) and non-compliant (≥ 84), the stepwise procedure sorted the following informative wavelengths: λ_{430}, λ_{580}, λ_{620} and λ_{650}. Based on these selected wavelengths, the subsequent discriminative CANDISC procedure separated the three classes according to two significant functions CAN1 and CAN2 (Wilks' λ = 0.159, approximate F value = 3.68, $df1 = 8$, $df2 = 76$, $P < 0.001$) accounted for 78.9 and 21.1% of the total variability, respectively. The low value of Wilks' λ and the significantly high D^2-Mahalanobis distances (from a minimum of 6.1 and a maximum of 13.7; $P < 0.001$) among the three quantitative classes indicated that the discriminant model was relatively robust and, therefore, reliable when used to predict the absence of PAs/PANOs. Indeed, the outcomes of the model showed a low capability to separate the compliant-class, especially in the comparison with the non-compliant-class.

To confirm the discriminative accuracy of the CDA algorithm, a confusion matrix was built by assigning each sample to the PAs/PANOs classes according to the shortest square Mahalanobis distance (Table 7). The results of this cross validation confirmed the capability of the CDA

Table 7. Confusion matrix and descriptive statistics of the three quantitative and four qualitative PAs/PANOs classes based on the results of the two canonical discriminating analyses (CDA).

Predicted	Quantitative classes			Predicted	Qualitative Classes				
	Actual				Actual				
	Absence	Compliant	Non-compliant		Absence	LSH-type	LS-type	L-type	S-type
Absence	**8**	3	2	Absence	**8**	0	1	0	0
Compliant	2	**8**	10	LSH-type	0	**3**	0	0	0
Non-compliant	0	2	**9**	LS-type	2	0	**7**	3	0
				L-type	0	0	1	**14**	0
				S-type	0	0	0	1	**3**
Total	10	13	21	**Total**	10	3	9	18	3
TP	8	8	9	TP	8	3	7	12	3
TN	29	19	21	TN	32	40	29	24	39
FP	5	12	2	FP	1	0	5	1	1
FN	2	5	12	FN	2	0	2	4	0
Sensitivity	0.80	0.62	0.43	Sensitivity	0.80	1.00	0.78	0.78	1.00
Specificity	0.85	0.61	0.91	Specificity	0.97	1.00	0.85	0.96	0.98
Accuracy	0.84	0.61	0.68	Accuracy	0.93	1.00	0.84	0.88	0.98
Precision	0.62	0.40	0.82	Precision	0.89	1.00	0.58	0.93	0.75
MCC	0.62	0.33	0.42	MCC	0.80	1.00	0.60	0.76	0.86

Quantitative classes: Absence, PAs/PANOs < 0.4 μg kg^{-1}; Compliant, $0.4 \leq$ PAs/PANOs < 84 μg kg^{-1}; PAs/PANOs ≥ 84 μg kg^{-1}; Qualitative classes: Absence, without the 17 monitored PAs/PANOs; L-type, lycopsamine-type; S-type, senecionine-type; LS-type, lycopsamine-senecionine-type; LSH-type, lycopsamine-senecionine-heliotrine-type; TP, true positive; TN, true negative; FP, false positive; FN, false negative; MCC, Matthews correlation coefficient. Bold values represent the samples classified correctly.

model to discriminate the pollens without PAs/PANOs. Specifically, only 0.20 of the samples of the absence-class were wrongly attributed to the compliant-class, as highlighted by the high MCC value (0.62). However, this supervised classifier model appeared to be unable to correctly distinguish the pollen samples according to the compliant or non-compliant amounts; between 0.38 and 0.57 of the samples were not assigned to their actual classes (Table 7). Moreover, for both classes, a relative high percentage of samples was recognised as pollen without alkaloids (absence-class).

The second CDA was built to identify the wavelengths as the ones primarily responsible for variability of the five qualitative PAs/PANOs classes (absence, L-, S-, LS- and LSH-type). The stepwise procedure sorted the nine most informative SCE-optical-light reflectance variables associated with the following wavelengths: λ_{400}, λ_{420}, λ_{430}, λ_{450}, λ_{460}, λ_{500}, λ_{570}, λ_{640} and λ_{700}. Such wavelengths were used to perform the CDA in order to evaluate the degree of dissimilarity among the five qualitative PAs/PANOs classes. This second CDA algorithm defined four significant functions, namely CAN1, CAN2, CAN3 and CAN4 (Wilks' $\lambda = 0.069$, approximate F value $= 3.29$, $df1 = 36$, $df2 = 114$, $P < 0.001$), which accounted for 68.9, 23.4, 5.3 and 2.4% of the total variability, respectively. According to the statistical parameters and the significantly high D^2-Mahalanobis distances (from a minimum of 4.0 and a maximum of 21.1; $P < 0.05$), this multivariate prediction model was more accurate in correctly recognising the absence-class from the others. In fact, the related confusion matrix based on the shortest D^2-Mahalanobis distances confirmed high predictive performance, especially for the specificity (0.97) and accuracy (0.93) in the case of the absence-class (Table 7). Moreover, L-type could be also discriminated due to its higher MCC value (0.76), as well as LSH- and S-type. The limited sampling number of the last two classes might reduce the reliability of the model. On the contrary, the LS-type seemed to be less effectively differentiated by the CDA model (MCC = 0.60).

The absence of PAs/PANOs is associated with a colour pattern that the supervised CDA model detected with a higher level of accuracy. Indeed, the presence of PAs/PANOs modified the wavelength absorbance pattern by inducing a reduction in both the L* and b* values. The outcomes of the CDA and the following cross-validation confirmed that the increase of the total PAs/PANOs amount was correlated with the decrease of L* and b* values. Moreover, the fact that there was an improvement in the classification performance among the qualitative classes highlighted a strong relationship between the different EFSA PAs/PANOs type and the pattern of the optical-light reflectance. For instance, bee pollen pellets from *Echium*, which mainly produce Echi/Echi-NO (L-type PAs/PANOs), had a characteristic deep purple colour. Thus, the presence of pollen from *Echium* in the samples could explain the diminishing in lightness and yellowness.

4. Conclusions

The validated LC-MS/MS method was suitable for quantification of 17 PAs/PANOs in bee pollen. PAs/PANOs were detected in 77% samples, of which 62% contained between 142 and 3356 μg kg^{-1}, amounts that could pose a risk for regular consumers. L-type PAs/PANOs were predominant, with Echi and Echi-NO present at the highest mean concentrations, while H-type compounds were less frequent and contributed with lower contents. The main outcomes of instrumental colour highlighted that grinding process of the pollen samples significantly increased lightness (L*) and yellowness (b*) values recorded with the SCI or SCE mode. In ground bee pollen samples, there was a significant relationship between the L* and b* colour coordinates and PAs/PANOs content. The ROC sorted L* and b* cut-offs to discriminate the samples based on the LOQ-TR (0.4 μg kg^{-1}) and EFSA-TR (84 μg kg^{-1}) gold standards of PAs/PANOs. Application of CDA seemed to be a reliable supervised statistical criterion to distinguish the pollens without PAs/PANOs (absence-class) from the compliant and non-compliant classes and from the LSH-, S- and L-type classes due to the optical-light reflectance pattern.

In summary, this study is the first that has established a significant correlation between the instrumental colour coordinates and the PAs/PANOs in bee pollen. The physical colorimetric approach coupled with multivariate statistical models could be a reliable and rapid preliminary

promising tool to distinguish whether bee pollens contain the 17 PAs/PANOs markers. This method could reduce the number of pollen samples that must be analysed by LC-MS/MS to confirm the effective presence of these alkaloids.

Declarations

Author contribution statement

Luciana De Jesus Inacio, Lorena Lucatello: Performed the experiments; Analyzed and interpreted the data; Wrote the paper.

Roberta Merlanti, Francesca Capolongo: Conceived and designed the experiments; Contributed reagents, materials, analysis tools or data; Wrote the paper.

Vittoria Bisutti: Performed the experiments; Analyzed and interpreted the data.

Barbara Contiero: Analyzed and interpreted the data; Wrote the paper.

Lorenzo Serva: Analyzed and interpreted the data.

Severino Segato: Analyzed and interpreted the data; Contributed reagents, materials, analysis tools or data; Wrote the paper.

Funding statement

This work was supported by the University of Padova (CPDA 158894/15 project) and FONDAZIONE CARIVERONA (call 2016-SAFIL project).

Competing interest statement

The authors declare no conflict of interest.

Additional information

No additional information is available for this paper.

References

BfR, 2011. Chemical Analysis and Toxicity of Pyrrolizidine Alkaloids and Assessment of the Health Risks Posed by Their Occurrence in honey. BfR. (Federal Institute for Risk Assessment). Opinion No. Retrieved from: https://www.bfr.bund.de/cm/349/chemical-analysis-and-toxicity-of-pyrrolizidine-alkaloids-and-assessment-of-the-health-risks-posed-by-their-occurence-in-honey.pdf.

Bisutti, V., Merlanti, R., Serva, L., Lucatello, L., Mirisola, M., Balzan, S., et al., 2019. Multivariate and machine learning approaches for honey botanical origin authentication using near infrared spectroscopy. J. Near Infrared Spectrosc. 27 (1), 65–74.

Boppré, M., Colegate, S.M., Edgar, J.A., Fischer, O.W., 2008. Hepatotoxic pyrrolizidine alkaloids in pollen and drying-related implications for commercial processing of bee pollen. J. Agric. Food Chem. 56 (14), 5662–5672.

Campos, M., Frigerio, C., Lopes, J., Bogdanov, S., 2010. What is the future of Bee-Pollen? J. ApiProduct ApiMed. Sci. 2 (4), 131–144.

Campos, M.G.R., Bogdanov, S., de Almeida-Muradian, L.B., Szczesna, T., Mancebo, Y., Frigerio, C., Ferreira, F., 2008. Pollen composition and standardisation of analytical methods. J. Apicult. Res. 47 (2), 154–161.

Chen, L., Mulder, P.P.J., Louisse, J., Peijnenburg, A., Wesseling, S., Rietjens, I.M.C.M., 2017. Risk assessment for pyrrolizidine alkaloids detected in (herbal) teas and plant food supplements. Regul. Toxicol. Pharmacol. 86, 292–302.

Chica, M., Campoy, P., 2012. Discernment of bee pollen loads using computer vision and one-class classification techniques. J. Food Eng. 112 (1–2), 50–59.

CIE, 1976. Colorimetrie. Commission Internationale de l'Eclairage 18th (36). London, UK.

Costa, M.C.A., Morgano, M.A., Ferreira, M.M.C., Milani, R.F., 2017. Analysis of bee pollen constituents from different Brazilian regions: quantification by NIR spectroscopy and PLS regression. LWT - Food Sci. Technol. 80, 76–83.

COT, 2008. COT Statement on Pyrrolizidine Alkaloids in Food. Committee on toxicity of chemicals in food, consumer products and the environment. Retrieved from: cot.food.gov.uk/pdfs/cotstatementpa200806.pdf. .

De-Melo, A.A.M., Estevinho, L.M., Moreira, M.M., Delerue-Matos, C., de Freitas, A.da S., Barth, O.M., de.Almeida-Muradian, L.B., 2018. A multivariate approach based on physicochemical parameters and biological potential for the botanical and geographical discrimination of Brazilian bee pollen. Food Biosci. 25 (July), 91–110.

De-Melo, A.A.M., Estevinho, M.L.M.F., Sattler, J.A.G., Souza, B.R., Freitas, A.da S., Barth, O.M., Almeida-Muradian, L.B., 2016. Effect of processing conditions on characteristics of dehydrated bee-pollen and correlation between quality parameters. LWT - Food Sci. Technol. 65, 808–815.

Denisow, B., Denisow-Pietrzyk, M., 2016. Biological and therapeutic properties of bee pollen: a review. J. Sci. Food Agric.

Dübecke, A., Beckh, G., Lüllmann, C., 2011. Pyrrolizidine alkaloids in honey and bee pollen. Food Addit. Contam. Part A Chemistry, Analysis, Control, Exposure and Risk Assessment 28 (3), 348–358.

Edgar, J.A., Colegate, S.M., Boppré, M., Molyneux, R.J., 2011. Pyrrolizidine alkaloids in food: a spectrum of potential health consequences. Food Addit. Contam. Part A Chemistry, Analysis, Control, Exposure and Risk Assessment 28 (3), 308–324.

EFSA, 2011. Scientific opinion on pyrrolizidine alkaloids in food and feed: EFSA Panel on Contaminants in the Food Chain (CONTAM). EFSA J. 9 (11), 1–134.

EFSA, 2017. Risks for human health related to the presence of pyrrolizidine alkaloids in honey, tea, herbal infusions and food supplements. EFSA J. 15 (7).

European Commission, 2002. Commission decision 2002/657/EC of 12 august 2002 implementing council directive 96/23/EC concerning the performance of analytical methods and the interpretation of results. Off. J. Eurp. Commun. 8–36. L221/8.

Ferrer, C., Lozano, A., Agüera, A., Jiménez Girón, A., Fernández-Alba, A.R., 2011. Overcoming matrix effects using the dilution approach in multiresidue methods for fruits and vegetables. J. Chromatogr. A 1218 (Issue 42), 7634–7639.

Gardana, C., Del Bo, C., Quicazán, M.C., Correa, A.R., Simonetti, P., 2018. Nutrients, phytochemicals and botanical origin of commercial bee pollen from different geographical areas. J. Food Compos. Anal. 73 (July), 29–38.

Hartmann, T., 1999. Chemical ecology of pyrrolizidine alkaloids. Planta 207 (4), 483–495.

Hosoya, Y., Shiraishi, T., Oshiro, M., Ando, S., Miyazaki, M., Powers, J.M., 2009. Effects of specular component on color differences of different filler type resin composites after aging. J. Dent. 37 (8), 585–590.

Kast, C., Kilchenmann, V., Reinhard, H., Bieri, K., Zoller, O., 2019. Pyrrolizidine alkaloids: the botanical origin of pollen collected during the flowering period of Echium vulgare and the stability of pyrrolizidine alkaloids in bee bread. Molecules 24 (12).

Kast, C., Kilchenmann, V., Reinhard, H., Droz, B., Lucchetti, M.A., Dübecke, A., et al., 2018. Chemical fingerprinting identifies Echium vulgare, Eupatorium cannabinum and Senecio spp. as plant species mainly responsible for pyrrolizidine alkaloids in bee-collected pollen. Food Addit. Contam. Part A Chemistry, Analysis, Control, Exposure and Risk Assessment 35 (2), 316–327.

Kempf, M., Heil, S., Haßlauer, I., Schmidt, L., von der Ohe, K., Theuring, C., et al., 2010. Pyrrolizidine alkaloids in pollen and pollen products. Mol. Nutr. Food Res. 54 (2), 292–300.

Kieliszek, M., Piwowarek, K., Kot, A.M., Błażejak, S., Chlebowska-Śmigiel, A., Wolska, I., 2018. Pollen and bee bread as new health-oriented products: a review. Trends Food Sci. Technol. 71, 170–180. November 2017.

Kostić, A., Milinčić, D.D., Petrović, T.S., Krnjaja, V.S., Stanojević, S.P., Barać, M.B., et al., 2019. Mycotoxins and mycotoxin producing fungi in pollen: Review. Toxins 11 (2).

Lucatello, L., Merlanti, R., Rossi, A., Montesissa, C., Capolongo, F., 2016. Evaluation of some pyrrolizidine alkaloids in honey samples from the veneto region (Italy) by LC-MS/MS. Food Anal. Methods 9 (6), 1825–1836.

Mattocks, A.R., Jukes, R., 1987. Improved field tests for toxic pyrrolizidine alkaloids. J. Nat. Prod. 50 (2), 161–166.

Molyneux, R.J., Gardner, D.L., Colegate, S.M., Edgar, J.A., 2011. Pyrrolizidine alkaloid toxicity in livestock: a paradigm for human poisoning? Food Addit. Contam. Part A Chemistry, Analysis, Control, Exposure and Risk Assessment 28 (3), 293–307.

Mulder, P.P.J., Sánchez, P.L., These, A., Preiss-Weigert, A., Castellari, M., 2015. Occurrence of pyrrolizidine alkaloids in food. EFSA Support. Publ. 12 (8).

Nuringtyas, T.R., Choi, Y.H., Verpoorte, R., Klinkhamer, P.G.L., Leiss, K.A., 2012. Differential tissue distribution of metabolites in Jacobaea vulgaris, Jacobaea aquatica and their crosses. Phytochemistry 78, 89–97.

Oplatowska, M., Elliott, C.T., Huet, A.C., McCarthy, M., Mulder, P.P.J., Von Holst, C., et al., 2014. Development and validation of a rapid multiplex ELISA for pyrrolizidine alkaloids and their N-oxides in honey and feed Rapid Detection in Food and Feed. Anal. Bioanal. Chem. 406 (3), 757–770.

Pereira De Melo, I.L., De Almeida-Muradian, L.B., 2010. Stability of antioxidants vitamins in bee pollen samples. Quim. Nova 33 (3), 514–518.

Picron, J., Herman, M., Van Hoeck, E., Goscinny, S., 2019. Monitoring of pyrrolizidine alkaloids in beehive products and derivatives on the Belgian market. Environ. Sci. Pollut. Control Ser. 1–16.

Salazar-González, C.Y., Rodríguez-Pulido, F.J., Terrab, A., Díaz-Moreno, C., Fuenmayor, C.A., Heredia, F.J., 2018. Analysis of multifloral bee pollen pellets by advanced digital imaging applied to functional food ingredients. Plant Foods Hum. Nutr. 73 (4), 328–335.

Stegelmeier, B., Edgar, J., Colegate, S., Gardner, D.R., Schoch, T.K., Coulombe, R.A., Molyneux, R.J., 1999. Pyrrolizidine alkaloid plants, metabolism and toxicity. J. Nat. Toxins 8 (1), 95–116.